Towards nonlinear photonic wires in Lithium Niobate

Hui Hu, Li Gui, Raimund Ricken, Wolfgang Sohler
Angewandte Physik, Department Physik, Universität Paderborn, 33098 Paderborn, Germany

ABSTRACT

The development of wafer-scale (3`` diameter) smart-cut lithium niobate (LN) single-crystal films of sub-micrometer thickness is reported. Z-cut LN wafers, implanted by high energy He-ions, are crystal-bonded to a SiO_2 layer on another Z-cut LN handle sample. The bonded pair of samples splits along the He-implanted layer by appropriate annealing. As this fabrication method is similar to the process widely used for silicon-on-insulator (SOI) fabrication, the resulting material is called LNOI.

Two different routes to develop periodically poled LNOI photonic wires are discussed. The first one starts with poling of planar LNOI samples; the photonic wires are fabricated afterwards by ICP-etching. The second one starts with the fabrication of LNOI photonic wires; they are "locally" poled afterwards. As both approaches were not yet successful, a PPLN-substrate was ion beam sliced to generate a planar periodically poled LNOI sample directly.

Using planar LNOI samples as starting material, high-quality photonic wires have been developed. The smallest structure has a cross-section of ~ 1 x 0.7 μm^2 only. Its optical properties with mode distributions, waveguide propagation losses, and group index were investigated. Moreover, the first periodically poled LNOI photonic wires were successfully fabricated, but not yet investigated optically. They are of great potential for second order nonlinear integrated optics.

Keywords: Lithium Niobate, photonic wire, periodic poling, nonlinear integrated optics.

1. INTRODUCTION

Optical waveguides of high refractive index contrast – such as the well developed Silicon-On-Insulator (SOI) "photonic wires" - can have a very small cross section (even below 1 μm^2) and also bending radius (~10 μm), enabling the development of ultra-compact photonic integrated devices and circuits [1]. A corresponding technology for Lithium Niobate (LN) is still in its infancy, though LN offers – in contrast to SOI - excellent electro-optic, acousto-optic, and nonlinear optical properties. Moreover, it can be easily doped with rare-earth ions to get a laser active material [2]. Therefore, LN photonic wires will enable the development of a wide range of extremely compact, active integrated devices, including electro-optical modulators, tuneable filters, nonlinear wavelength converters, and amplifiers and (tuneable) lasers of different types. In particular, periodically poled LN (PPLN) photonic wires are ideal candidates for extremely efficient nonlinear optical devices for wavelength conversion and all-optical signal processing.

Thin (sub-micrometer) LN films of high refractive index contrast can be the starting material to fabricate LN photonic wires. Using "ion beam slicing" technology, free-standing LN films with areas of several cm^2 were successfully fabricated and devices were demonstrated [3]. Crystal ion beam slicing was combined with direct bonding to fabricate LN films on SiO_2 of an area of ~ $1cm^2$ [4]. Using benzocyclobutene (BCB) as cladding layer, LN films of a size of several cm^2 were realized and electro-optical tunable micro-ring resonators were reported [5]. We have recently developed a full wafer technology to fabricate single crystalline LN-layers of sub-micrometer thickness on a vacuum-deposited SiO_2-layer on a LN-substrate [6]. In contrast to the BCB bonded material, annealing at much higher temperatures is possible. High temperature annealing can minimize ion-implantation induced material damage and helps to recover electro- and nonlinear optical properties. Moreover, high temperature annealing contributes significantly to a reduction of the surface roughness of LN ridge guides.

Integrated Optics: Devices, Materials, and Technologies XIV, edited by Jean-Emmanuel Broquin, Christoph M. Greiner,
Proc. of SPIE Vol. 7604, 76040R · © 2010 SPIE · CCC code: 0277-786X/10/$18 · doi: 10.1117/12.842674

For efficient second order nonlinear optical interactions, (quasi-) phase-matching (QPM) is required. In LN QPM can be achieved by a periodic ferroelectric domain inversion. However, periodic poling of LN photonic wires is still a great challenge to the fabrication technique and has not yet been demonstrated up to now.

We report in this paper our recent progress towards the fabrication of periodically poled photonic wires in LN. In the first chapter the development of different LN-On-Insulator (LNOI) structures is presented, partially with metallic electrodes incorporated. Different approaches to realize a periodic domain inversion will be discussed in the second chapter. The fabrication and the optical properties of mono-domain LNOI photonic wires are presented in the third chapter. Moreover, some results on the first periodically poled LNOI photonic wire are given.

2. WAFER-SCALE (SMART-CUT) LITHIUM NIOBATE ON INSULATOR (LNOI)

In the following, the full-wafer process to fabricate a single crystalline LN-layer of sub-micrometer thickness on a vacuum-deposited SiO_2-layer on a LN-substrate is briefly described. To enable a periodic poling of the LN-layer, also different sandwich structures with a thin metal electrode either underneath the SiO_2 layer or underneath the LN-film have been fabricated. Even LNOI with a MgO:LN-film on SiO_2 on a LN-substrate has been demonstrated.

2.1 Schematic full wafer fabrication

The special "smart cut" process, widely used for the fabrication of a thin single crystalline Silicon film on an amorphous SiO_2-layer on a Silicon-substrate, better known as Silicon-On-Insulator (SOI) [7], was used for the fabrication of LN-films on SiO_2 on a LN-substrate. Due to this analogy we introduced for our sandwich structure the name LNOI. Such crystal bonded layer structures have been pioneered by the groups of Osgood [8] and Günter [9] on smaller substrates.

Our full wafer fabrication process is schematically sketched in Fig. 1. At first, a Z-cut LN wafer of 3`` diameter is implanted by 250 keV or 350 keV He-ions, respectively, with a dose of 4×10^{16} ions/cm^2 forming an amorphous layer at about 760 nm or 1040 nm underneath the surface. Another Z-cut LN handle sample is coated by a SiO_2-layer of 1.8 µm thickness by plasma enhanced chemical vapor deposition (PECVD), and then annealed at 450 ^oC for 8 hours to drive off the gases trapped in the oxide layer. With a chemical mechanical polishing (CMP) process, the surface roughness is reduced from about 6 nm to 0.35 nm enabling direct wafer bonding. The bonded pair of samples is then annealed to improve the bonding strength; by a further increase of the temperature to 228 ^oC for 2 hrs the sample splits along the He implanted layer. Afterwards, it is annealed at 450 ^oC for 8 hours, before the LNOI-surface is polished by another CMP-process. The final thickness of the LN-layer typically is 760 nm.

We also fabricated sandwich structures with a metal film underneath or on top of the SiO_2-layer before crystal bonding.

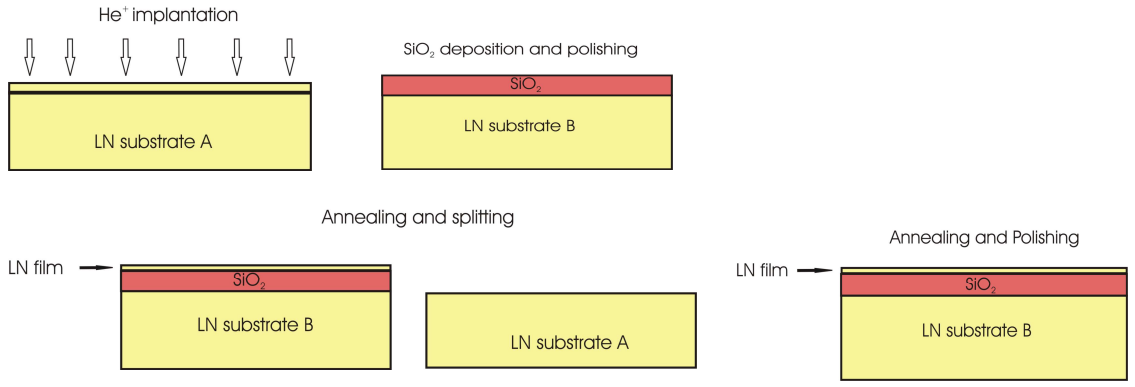

Figure 1: Fabrication scheme of LNOI: a "smart cut" single crystalline LN-film of sub-micrometer thickness is crystal-bonded to a SiO_2/LN substrate (see also text).

2.2 LN-film/SiO_2/LN-substrate

Fig. 2 presents a LNOI wafer of 3 inch diameter fabricated by the process sketched above. The good homogeneity of the interference colors underlines the homogeneity of the fabrication process. A part of such a sample was used to develop LNOI photonic wires as described in the third chapter.

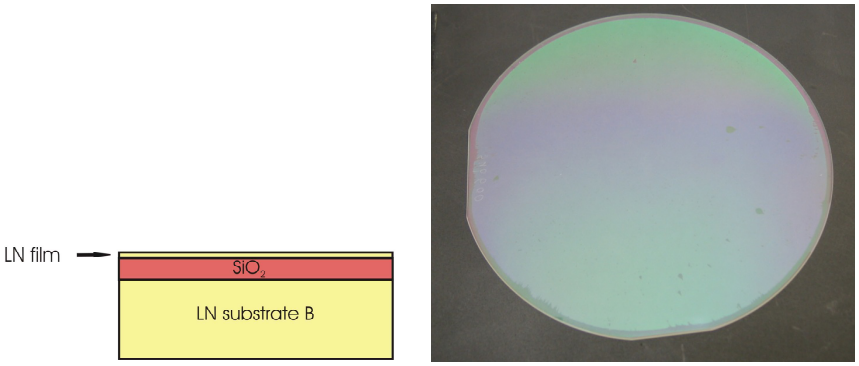

Figure 2: Schematic cross-section (left) and photograph (right) of a LNOI-wafer of 3`` diameter, consisting of a 760 nm thick single crystalline LN-film crystal bonded on a 1.3 µm thick SiO_2-layer deposited by PECVD on a LN-substrate.

2.3 MgO:LN-film/SiO_2/CrAuCr/LN-substrate

Fig. 3 shows the result of experiments to fabricate a LNOI wafer of 3 inch diameter with a MgO-doped LN thin film on top and a Cr-Au-Cr metal electrode underneath the SiO_2-layer. The idea was to take advantage of the lower coercive field of MgO:LN and to facilitate (light assisted) electric field poling via a second electrode on top of the LNOI-surface. However, corresponding experiments failed up to now; it seems, that the required conductivity of the SiO_2-layer is too low to allow the flow of the poling current. On the other hand, some spontaneously generated micro-domains could be observed after the final annealing and polishing processes (see Fig. 3).

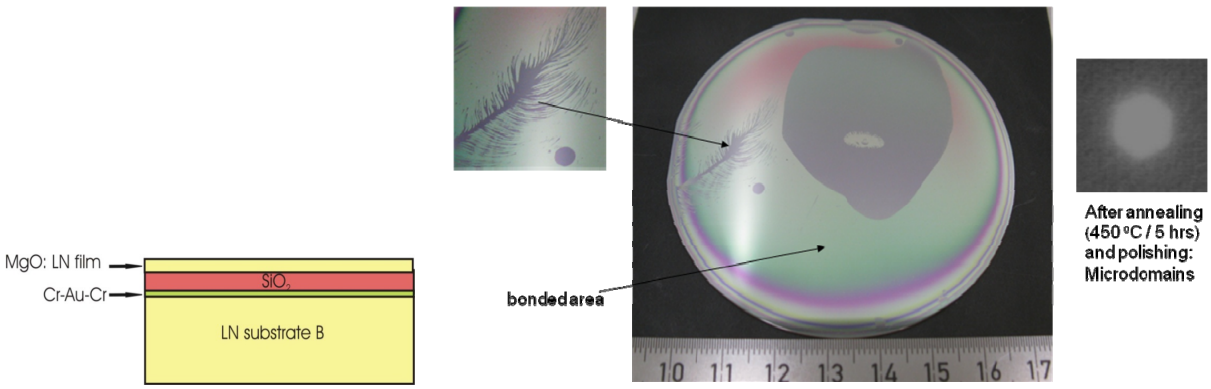

Figure 3: Schematic cross-section (left) and photograph (right) of a LNOI-wafer of 3`` diameter, consisting of a 1040 nm thick single crystalline MgO:LN-film crystal bonded on a 1.3 µm thick SiO_2-layer deposited by PECVD on a thin (~40 nm) evaporated Cr-Au-Cr-electrode on a LN-substrate. On the outer right: spontaneously formed micro-domain of inverted polarization.

2.4 LN-film/Ti/SiO_2/LN-substrate

Also sandwich structures with a thin Ti-film as poling electrode on top of the SiO_2-layer have been developed (see Fig. 4). They are currently investigated to get electric field poling via a second electrode on top of the LNOI-surface. Poling voltages of a few tens of Volts should be sufficient to overcome the coercive field.

A metal layer of Ti has been chosen to allow a thermal oxidation after poling. We expect that the resulting TiO_2-layer of high refractive index would only slightly modify the LNOI waveguide characteristics and would avoid ohmic losses for guided wave propagation.

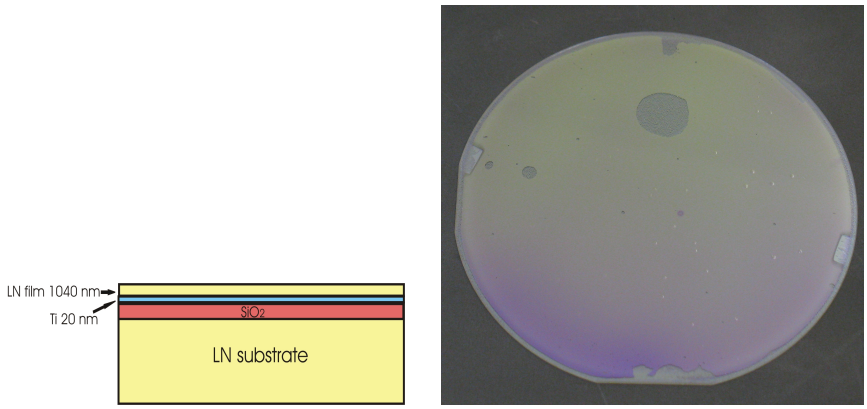

Figure 4: Schematic cross-section (left) and photograph (right) of a LNOI-wafer of 3`` diameter, consisting of a 1040 nm thick single crystalline LN-film crystal bonded on a 20 nm thick evaporated Ti-electrode on a 1.3 µm thick SiO_2-layer deposited by PECVD on a LN-substrate. Here, the upper surface of the LN-film is not yet polished after splitting.

2.5 Periodically poled LN-film/SiO_2/LN-substrate

If a PPLN-substrate is ion beam sliced and used as substrate A (see Fig. 1) in the fabrication process, a periodically poled LNOI-film can be fabricated. This was very recently demonstrated with a small sample, not yet with the full-wafer process.

3. POLING TECHNOLOGIES

We follow two different strategies to develop periodically poled LNOI photonic wires. The first one starts with poling of planar LNOI samples to do the photonic wire fabrication afterwards by ICP-etching. The second one starts with the fabrication of photonic wires from planar LNOI samples and does the periodic poling afterwards. In the following, the two corresponding poling procedures are briefly described.

3.1 (Conventional) electric field poling

The well-known standard method of periodical poling of bulk LN-wafers (e.g. of 500 µm thickness) is sketched in Fig. 5 together with an example. Z-cut samples have to be used with a periodic (liquid or metallic) electrode on one surface and a planar electrode on the other. By applying an electric field surpassing the coercive field of LN, ferroelectric domain inversion can be obtained either in a pulsed or quasi-cw mode of operation. However, the example presented in Fig. 5 simultaneously shows the limitation of this process. With a substrate of 500 µm thickness a very regular domain structure with periodicities down to 1.7 µm could be obtained near the surface but no longer through the whole substrate. This was made visible by cutting the crystal perpendicular to the Y-axis, polishing, and slightly etching the new surface. This procedure revealed that only few domains grew through the whole crystal. In general: the smaller the periodicity is, the more difficult is a reliable fabrication. Therefore, our fabrication of periodically poled LNOI with a smart cut of bulk PPLN (see section 2.5) is limited to periodicities well above 1 µm.

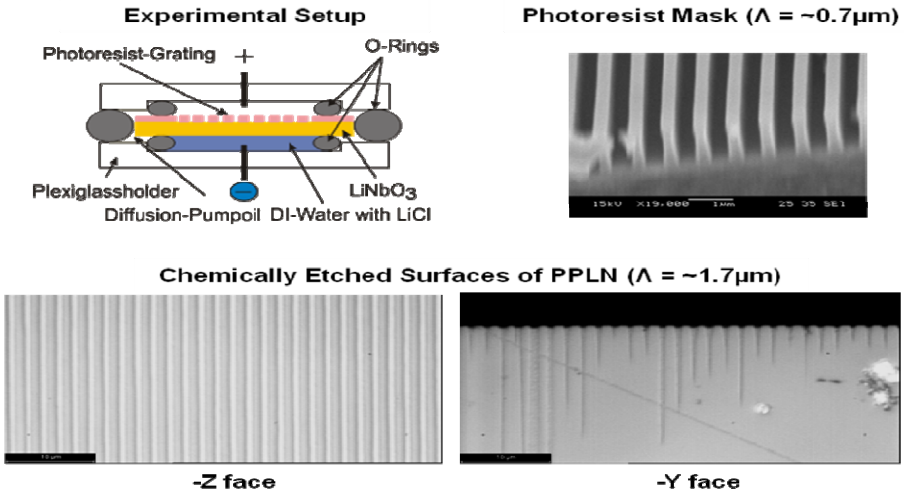

Figure 5: Scheme of the experimental set-up for periodical poling of 500 µm thick LN-samples (upper left). A photoresist mask can be designed for periodicities well below 1 micrometer (upper right). Successful poling could be demonstrated with periodicities down to 1.7 µm (lower left: micrograph of the preferentially etched Z-face); however, the growth of the domains into the body of the LN-sample was irregular (lower right: micrograph of etched Y-face of the sample after cutting).

The generation of smaller domains requires thinner substrates for poling. Therefore, we are confident that LNOI-wafers are ideal candidates for the fabrication of periodically poled structures even with sub-micrometer periodicity. Such fine structures are e.g. required for quasi phase-matched nonlinear interactions in backward direction.

To enable poling of planar LNOI, we developed two different structures with a metallic electrode incorporated (see Figs. 3 and 4). However, up to now we were not able to demonstrate controlled poling. We believe that a small electrical conductivity of the SiO_2-layer is necessary, to allow the flow of a poling current. Such a conductivity might be obtained by a slight doping of the SiO_2-layer. Also the alternative structure of Fig. 4 (see also Fig. 6) did not yet enable successful poling, though a current flow was observed. Structure and process are currently investigated to learn to know the reason for this unexpected behavior. On the other hand, a successful oxidation of the Ti-layer between LN- and SiO_2-film could already be demonstrated, but light propagation in the thus modified (planar) LNOI-waveguide has still to be investigated.

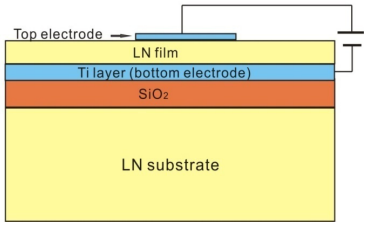

Figure 6: Schematic cross-section of a LNOI-structure with electrodes for electric field poling.

3.2 Local periodic poling

Recently, we have developed a "local" poling technique for Ti:LN ridge guides of e.g. 9 x 4 μm^2 cross-section on X-and Y-cut LN [10]. It was possible to define periodic electrodes on both sides of the ridge. Fig. 7 presents a scheme of the comb like electrode structure. Since the ridge guide has width of 9 µm, a relatively low poling voltage is needed for "local" micro-domain inversion - in the body of the ridge only. Due to the coercive field of LN of ~20 kV/mm, domain inversion should start at ~ 166 V. Most times, due to the imperfection of the electrodes, the actual applied voltage had to be higher.

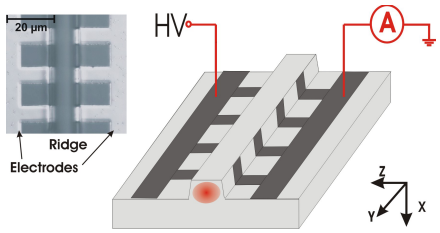

Figure 7: Right: Scheme of the poling configuration for a ridge on X-cut LN. Left: Top view (micrograph) of the electrodes of 16.6 µm periodicity on both sides of a 9 µm wide ridge.

To reveal the shape and uniformity of the ferroelectric micro-domains in the periodically poled ridge, the sample was selectively etched, and then observed from top using optical microscopy. Fig. 8(a) shows the upper surface of an etched ridge on an X- cut substrate. A periodical modulation of the side walls is seen, as +Z- and –Z-faces are etched with different velocities.

Afterwards the sample has been cut through the body of the ridge as shown in Fig. 8 (d) and etched again in $HF:HNO_3$. In this way the +Z- and –Z-faces of the periodical domain structure can be observed on the sidewall and in the body of the ridge. Due to the different etching rates the inverted domains become visible (Figs. 8 (b,c)). A nearly hexagonal shape is observed as marked with white dash lines in Fig. 8 (c). The depth of the domains (in X-direction) corresponds to the height of the ridge as expected.

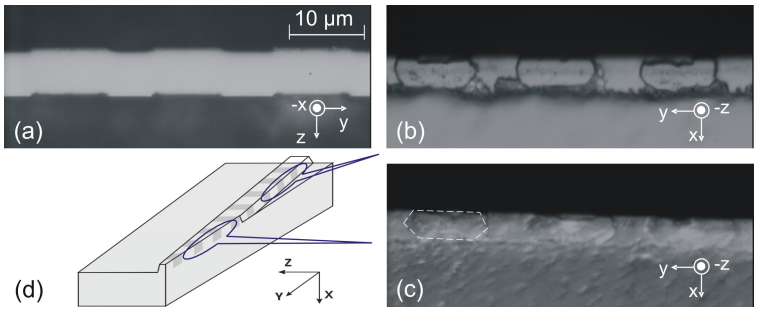

Figure 8: Selectively etched, periodically poled ridge on X-cut LN. (a) Top view. (b) Side view. (c) Side view after cutting the ridge. (d) Cutting scheme.

The same poling procedure should be possible for LNOI photonic wires. However, if fabricated on Z-cut material as discussed above for the wafer-scale planar LNOI, a different electrode structure would be required with one electrode on top of the ridge and one (or two) on both sides of the ridge on the surface of the substrate. Such a structure is much more difficult to be fabricated. The development of periodically poled photonic wires on X-cut LNOI might be more promising; however, this material is not yet available.

4. LNOI PHOTONIC WIRES

Recently, high-quality photonic wires have been developed, using LNOI-samples as shown above in Fig. 2 as starting material. The smallest photonic wires made up to now have cross-section dimensions of ~ 1 x 0.7 μm^2 only. Their fabrication is briefly described in the first section, followed by a discussion of the optical properties of these waveguides. More details can be found in [11]. In the third section, the first periodically poled LNOI photonic wire is presented, successfully fabricated just before “Photonics West 2010”; its optical properties have not yet been investigated.

4.1 Fabrication

For the fabrication of photonic wires, a LNOI sample was used, which consists of a 730 nm thick single crystalline LN layer directly bonded to the surface of a 1.3 µm thick SiO_2 layer.

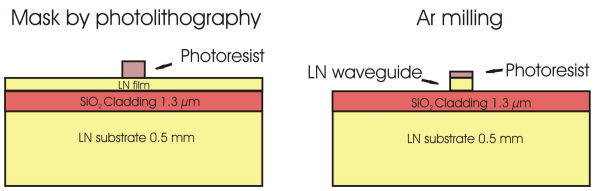

Figure 9: Schematic diagrams of the cross-section of the LNOI sample (left) used to fabricate photonic wires (right) by Ar-milling.

The fabrication process is schematically shown in Fig. 9. Photoresist (OIR 907-17) stripes of 1.7 μm thickness and 1 - 7 μm width were defined by photolithography as the etch mask. The resist was annealed at 120 °C for 1 hour to improve the etching selectivity. Subsequently, the sample was etched by Ar milling for 60 min in an Oxford Plasmalab System100 with 100 W RF power inductively coupled into the plasma (ICP) and 70 W RF power coupled to the sample table. The resulting etch depth was 460 nm. A longer etching time is needed to remove the LN layer completely. Fig. 10 shows scanning electron microscope (SEM) pictures of a ridge guide of 1 μm top width. The dark stripe underneath is the SiO_2 cladding. On both sides of the ridge, etched trenches can be observed, resulting from additional etching by ions reflected by the angled walls of the ridge. Their slope of ~ 27° (with respect to the vertical direction) is determined by the dependence of the etching rate on the incident angle of the ion beam. Finally, the end faces of the sample were carefully polished to enable efficient end-fire coupling of light; the length of the sample was 3 mm.

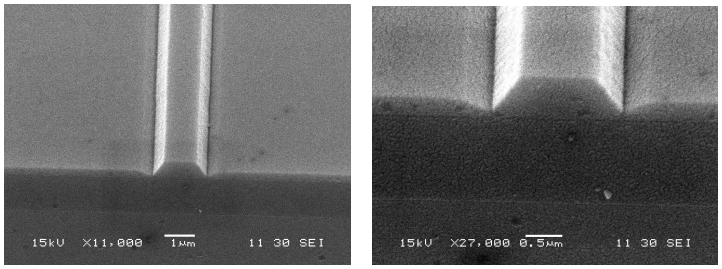

Figure10: SEM pictures of micro-channel ridge guides (photonic wires) of 1 μm top width. The trenches on both sides of the ridges reach near the surface of the SiO_2 buffer layer.

4.2 Optical properties

The LNOI photonic wires were investigated in the 1.55 μm wavelength range. The mode distributions were measured and compared with modeling results. Using the resonator method the propagation losses were determined. This method requires the knowledge of end face reflectivity of the waveguide, which was calculated by a finite difference method for both polarizations and as function of the waveguide width. Moreover, the group index of the waveguides was measured and also compared with modeling results.

a. Mode distributions

The light from a tunable laser diode was coupled to the waveguides by a 60× / 0.8 objective with an estimated coupling efficiency of about 40 % and 30 % to the fundamental mode of the photonic wires of 2 and 1 μm top width, respectively. On the output side a 100× / 0.9 objective magnified the near field distribution of the guided mode to form an image of maximum spatial resolution (~ 1.1 μm) on the camera. The recorded data were transmitted to a computer for further signal processing.

The mode distributions were measured as function of the waveguide width and of the polarization, and compared with simulated distributions calculated with a full-vectorial finite difference method. The waveguide profile assumed for the calculations is indicated in Figures 11 and 12. In the following, mode distributions for the ridge guides of 2 and 1 μm top width are presented as examples.

Despite the small cross section dimensions, both structures support - according to the modeling results - not only the fundamental, but at least also the second order mode at 1.55 µm wavelength (see Figs. 11 and 12). However, by a careful adjustment of the input laser beam, the fundamental mode could be selectively excited (though it was difficult to control the selective excitation with the objective of limited resolution). Moreover, the remaining thin LN films of 270 nm thickness on both sides of the photonic wires formed a planar waveguide for qTE polarization.

Figure 11 shows the measured mode distribution for quasi TM-polarization (qTM) at the output of a 2 µm wide channel (left) together with a corresponding modeling result (middle). In view of the finite spatial resolution of the imaging system, the agreement is reasonable. The calculated second order mode is displayed on the right of Figure 11.

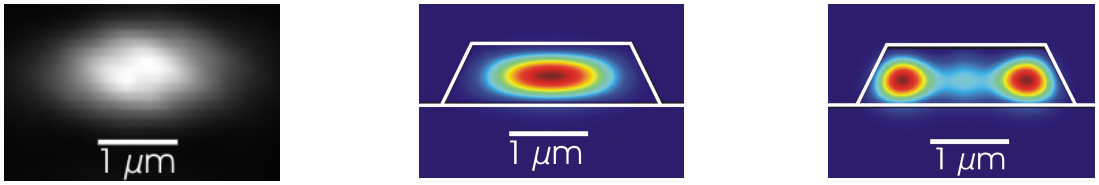

Figure 11: Measured (left) and calculated (middle) intensity distribution of the fundamental mode in a photonic wire of 2 µm top width (qTM-polarization; λ = 1.55 µm). The intensity distribution of the simulated second order mode is shown on the right. The profile, used for the simulations, is indicated (middle and right).

Figure 12 shows the measured (left) and calculated (middle) distribution of the fundamental quasi TE mode (qTE) in a photonic wire of 1 µm top width. Again, in view of the finite spatial resolution of the imaging system, the agreement is reasonable. The mode cross section is about 0.5 μm^2 (product of FWHM in horizontal and vertical directions of the calculated distribution), more than one order of magnitude smaller than the mode size of about 25 μm^2 in a conventional Ti-indiffused strip guide of 7 µm width. The corresponding data for qTM polarization are 0.4 μm^2 and 16 μm^2. Therefore, such photonic wires are ideal candidates to develop nonlinear devices of high efficieny. Moreover, high bending radii become possible without inducing excess bending losses. The calculated second order mode is displayed on the right. To obtain a mono-mode photonic wire, a smaller width or steeper walls are needed.

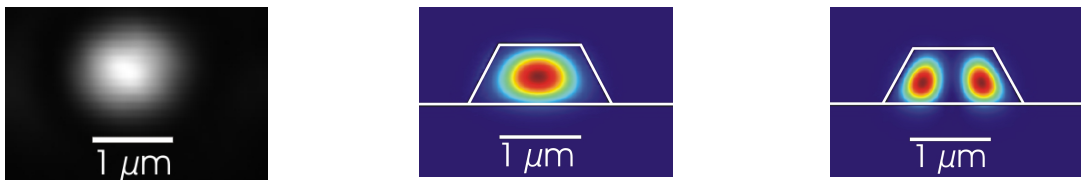

Figure 12: Measured (left) and calculated (middle) intensity distribution of the fundamental mode in a channel waveguide of 1 µm top width (qTE-polarization; λ = 1.55 µm). The intensity distribution of the simulated second order mode is shown on the right. The profile, used for the simulations, is indicated (middle and right).

b. Propagation losses and end face reflectivities

As the polished waveguide end faces represent mirrors of considerable reflectivity R, waveguide cavities of low finesse are formed. By analyzing the contrast K of the cavity resonances, measured as function of the wavelength, the mode propagation losses α was determined. This method is independent on the mode excitation efficiency. α, R* and K are defined by the following equations [12]:

$$\alpha = 4.34\ (\ln R - \ln R^*)/L \qquad \text{with } R^* = (1-\sqrt{(1-K^2)})/K \text{ and } K = (I_{max} - I_{min}) / (I_{max} + I_{min})$$

However, due to the small waveguide cross section, the modal reflectivity R (ratio of reflected mode power to the incident mode power) can no longer be approximated by the Fresnel result for plane waves of normal incidence at a LN-air interface (~14 %) as usually done for weakly guiding structures. The actual value of R is required to enable a correct

evaluation of the propagation losses. Therefore, and as a mode-selective measurement is difficult, R was calculated by a 3-dimensional finite difference time domain (FDTD) solver. An auto-non-uniform mesh was used with 30 nm maximum step size in the LN waveguide region, with uniaxial perfect matched layer (PML) boundary conditions. The result is presented in Fig. 13 as function of the top width of the ridge guides of 730 nm thickness. The slope of the ridges was kept constant. With increasing waveguide width, the end face reflectivity R approaches polarization dependent limits with a significantly higher reflectivity for qTE than for qTM. Due to the waveguide thickness of 730 nm only, $\Delta R = R_{qTE} - R_{qTM}$ converges to ~ 11 %; this figure shrinks to ~ 1 % with increasing thickness, determined by the birefringence of LN alone. With decreasing waveguide width (at 730 nm thickness), ΔR also shrinks to small figures, as qTE and qTM modes become nearly degenerate.

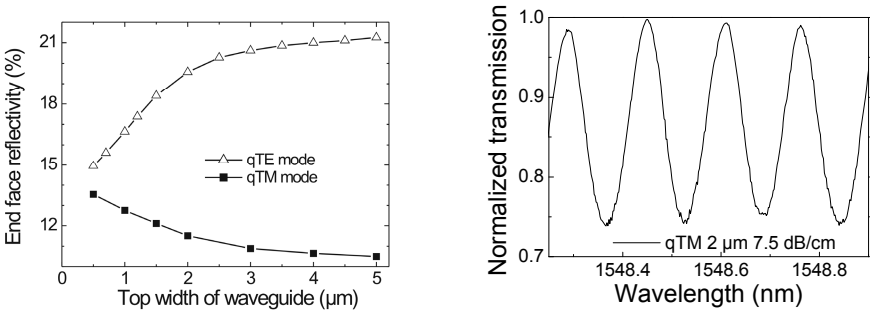

Figure 13: Left: Calculated end face reflectivities of the fundamental modes of qTE and qTM polarization, respectively, versus the top width of LN photonic wires of 730 nm thickness. Right: Normalized transmission in qTM polarization of a channel guide of 2 μm top width as function of the wavelength.

The simulated end face reflectivities allowed determining the waveguide propagation losses from the contrast of the cavity resonances according to the formula (1) given above. Figure 13 shows on the right as an example the measured normalized transmission in qTM polarization of a photonic wire of 2 μm top width as function of the wavelength. A propagation loss of 7.5 dB/cm was evaluated. For qTE polarization, the loss is 6.3 dB/cm. The corresponding results for a photonic wire of 1 μm top width are 9.9 dB/cm and 12.9 dB/cm for qTM and qTE polarization, respectively. The larger qTE losses in the narrower wire may result from some coupling to the planar (single polarization) waveguides on both sides of the channel.

The losses very likely arise from scattering by the residual roughness of all four walls of the ridge. Losses due to a coupling of the propagating mode across a 1.2 μm thick SiO_2 layer to the substrate should be negligible (< 0.05 dB/cm), according to the calculations with a fully vectorial finite difference mode solver.

c. Effective and group indices

The waveguide mode dispersion is determined by the material dispersion of core and cladding materials and by the waveguide dimensions. Due to the high index contrast of the photonic wires and their small cross section dimensions, the effective index of refraction n_{eff} varies considerably as function of the wavelength between the bulk index of LN and that of SiO_2. It was calculated by the finite difference method for the fundamental qTE- and qTM-modes, respectively, and for several waveguide widths; some results are displayed in Figure 14 together with the dispersion of bulk LN and SiO_2.

Whereas an effective mode index n_{eff} is difficult to measure, the group index n_g can be derived in a small wavelength range from the measured transmission spectra of the waveguides (see Figure 12): $n_g = \lambda^2 / (2 \cdot L \cdot \Delta\lambda)$; L is the waveguide length and Δλ is the wavelength difference of neighboring resonances. In addition, the group index was also calculated as $n_g = n_{eff} - \lambda \cdot (dn_{eff} / d\lambda)$; measured and calculated results are shown in Figure 14 for the fundamental modes of qTE and qTM polarization, respectively. For comparison, also the calculated group index of bulk LN is shown derived from a Sellmeier equation describing the dispersion of bulk LN.

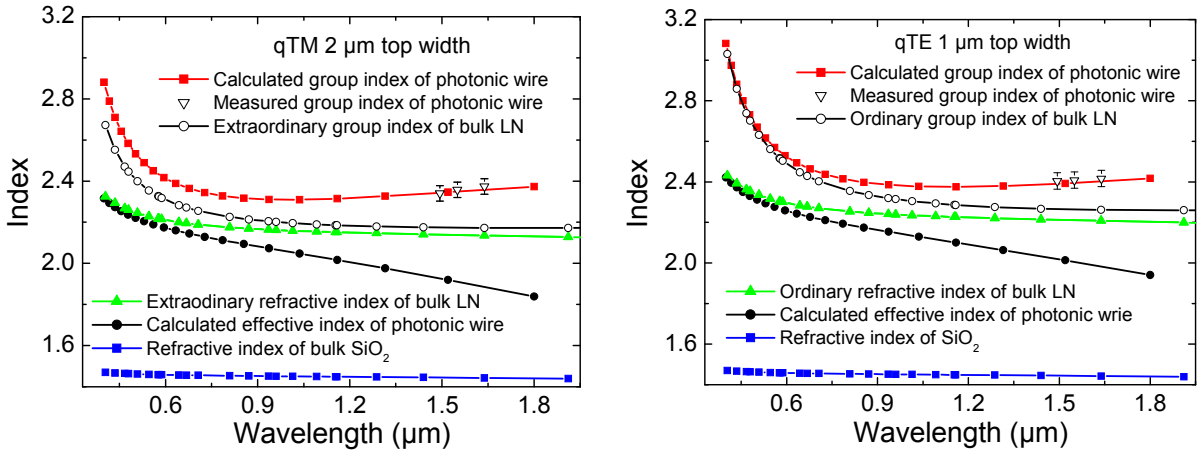

Figure 14: Calculated effective and group indices for the fundamental modes of qTM and qTE polarization in photonic wires of 2 µm and 1 µm top widths, respectively, versus the wavelength. The measured group indices of photonic wires, the calculated group indices of bulk LN, and the refractive indices of bulk LN and SiO_2 are shown as well for comparison.

The effective indices of refraction vary between the bulk indices of LN and SiO_2; the longer the wavelength and the smaller the waveguides are, the lower the effective indices become due to a decreasing mode confinement. At shorter wavelengths, the mode is more and more confined in the LN core of the waveguide and n_{eff} approaches the (polarization dependent) bulk index of LN. The group indices for light propagation in the photonic wires are substantially larger than for light propagation in bulk LN, reflecting the influence of the small waveguide dimensions. They even allow adjusting a group index dispersion close to zero in the 1.5 µm wavelength range, which is of interest for optical communication devices.

4.3 The first periodically poled LNOI photonic wire

Starting from a periodically poled planar sample (and following the first strategy sketched in chapter 3), several periodically poled LNOI photonic wires of different width (1 – 7 µm) and of 9 µm periodicity have been fabricated by ICP-etching. The fabrication was very similar to the procedure described in section 4.1. However, the thickness of the remaining LN-film on both sides of the ridge (separated again by etched trenches) is somewhat larger than before; it is now about 390 nm. Fig. 15 shows as example a periodically poled LNOI wire of 1 µm width, 320 nm thickness of the ridge, and of a length of 3 mm. As the domain structure was hardly visible in SEM micrographs, an optical micrograph is also presented taken with a differential interference contrast microscope. After some contrast enhancement, the domain grating is clearly visible not only in the remaining LN-film on both sides of the ridge, but also in the photonic wire itself.

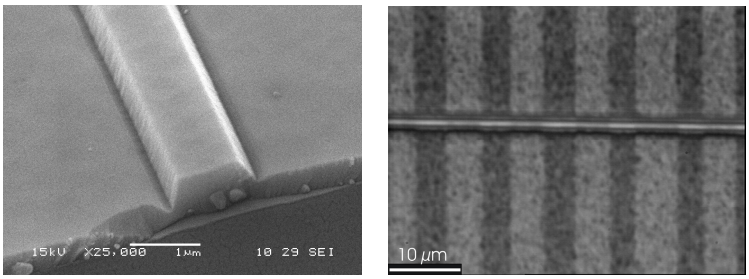

Figure 15: SEM micrograph (left) and optical micrograph (right) of a periodically poled LNOI photonic wire of 1 µm top width. The periodicity of the ferroelectric domain grating is 9 µm.

5. CONCLUSIONS

The recent development of wafer-scale high-index contrast LNOI has been described. Similar to SOI, it might become a new platform for ultra-compact integrated photonic devices and circuits. Various approaches are currently investigated to periodically pole the thin LN-films. Up to now, just ion-beam slicing of PPLN was successful to fabricate periodically poled LNOI as starting material for the development of photonic wires with a nonlinear grating.

Using LNOI-samples high-quality, photonic wires have been developed. The smallest photonic wires, made up to now, have cross-section dimensions of ~ 1 x 0.7 μm^2 only. Their fabrication has been briefly described, followed by a discussion of the optical properties of these waveguides. Due to the ultra-small mode size, periodically poled photonics wires would be most attractive for the development of second order nonlinear devices of highest efficiency.

The first periodically poled LNOI photonic wires, successfully fabricated in the last days, have been presented. They have a domain periodicity of 9 µm. Smaller periodicities will be possible, when one of the two routes to poling sketched in chapter 3, is successful. In particular, sub-micrometer ferroelectric domain structures would be extremely attractive enabling the development of devices with backward nonlinear coupling.

Acknowledgement:

This work was funded by the Deutsche Forschungsgemeinschaft (DFG) within the framework of the project "Materials World Network: Nanoscale Structure and Shaping of Ferroelectric Domains". Moreover, additional support by the DFG-Graduiertenkolleg "Micro- and Nanostructures in Optoelectronics and Photonics" at the University of Paderborn is gratefully acknowledged.

REFERENCES

[1] Kokubun, Y., "High Index contrast optical waveguides and their applications to microring filter circuit and wavelength selective switch," IEICE TRANS. ELECTRON., E90–C, (5), 1037-1045 (2007)

[2] Sohler, W., Das, B., Dey, D., Reza, S., Suche, H. and Ricken, R., "Erbium-doped lithium niobate waveguides lasers," IEICE Trans. Electron. E. 88-C (5), 990-997 (2005)

[3] Djukic, D., Cerda-Pons, G., Roth, R. M., Osgood, Jr., R. M., Bakhru, S. and Bakhru, H., "Electro-optically tunable second-harmonic-generation gratings in ion-exfoliated thin films of periodically poled lithium niobate," Appl. Phys. Lett. 90, 171116 (2007)

[4] Rabiei, P. and Günter, P., "Optical and electro-optical properties of sub-micrometer lithium niobate slab waveguides prepared by crystal ion slicing and wafer bonding," Appl. Phys. Lett., 85(20), 4603-4605 (2004)

[5] Guarino, A., Poberaj, G., Rezzonico, D., Degl'innocenti, R. and Günter, P., "Electro–optically tunable microring resonators in lithium niobate," Nature Photonics 1, 407-410 (2007)

[6] Hu, H., Ricken, R. and Sohler, W., "Large area, crystal-bonded $LiNbO_3$ thin films and ridge waveguides of high refractive index contrast," Proc. Topical Meeting "Photorefractive Materials, Effects, and Devices - Control of Light and Matter" (PR`09), Bad Honnef, Germany 2009

[7] Bruel, M., "Silicon on insulator material technology", Electron. Lett., 31, 1201-1202 (1995)

[8] Levy, M., Osgood Jr., R. M., Liu, R., Cross, L. E., Cargill III, G. S., Kumar, A. and Bakhru, H., "Fabrication of single-crystal lithium niobate films by crystal ion slicing," Appl. Phys. Lett., 73(16), 2293-2295 (1998)

[9] Poberaj, G., Koechlin, M., Sulser, F., Guarino, A., Hajfler, J. and Günter, P. "Ion-sliced lithium niobate thin films for active photonic devices," Opt. Mater. 31, 1054-1058 (2009)

[10] Gui, L., Hu, H., Garcia-Granda, M. and Sohler, W., "Local periodic poling of ridges and ridge waveguides on X- and Y-cut $LiNbO_3$ and its application for second harmonic generation," Opt. Express 17(5), 3923-3928 (2009)

[11] Hu, H., Ricken, R. and Sohler, W., "Lithium niobate photonic wires," Opt. Express 17(26), 24261-24268 (2009)

[12] Regener, R. and Sohler, W., "Loss in low-finesse Ti:$LiNbO_3$ optical waveguide resonators," Appl. Phys. B **36**(3), 143–147 (1985)